Ultrasonics Sonochemistry 79 (2021) 105756

Contents lists available at ScienceDirect

Ultrasonics Sonochemistry

journal homepage: www.elsevier.com/locate/ultson

Emulsion gels stabilized by soybean protein isolate and pectin: Effects of high intensity ultrasound on the gel properties, stability and β-carotene digestive characteristics

Xin Zhang, Xing Chen, Yuhang Gong, Ziyue Li, Yanfei Guo, Dianyu Yu *, Mingzhe Pan *

School of Food Science, Northeast Agricultural University, Harbin, 150030, China

ARTICLE INFO

Keywords:
High intensity ultrasound
Emulsion gel
Thermal stability
β-carotene
In vitro digestion

ABSTRACT

In this study, soybean protein isolate (SPI) and pectin emulsion gels were prepared by thermal induction, and the effects of high intensity ultrasound (HIU) at various powers (0, 150, 300, 450 and 600 W) on the structure, gel properties and stability of emulsion gels were investigated. Fourier transform infrared spectroscopy (FTIR) and X-ray diffraction (XRD) showed that the interaction between SPI and pectin was enhanced and the crystallinity of the emulsion gels was changed due to the HIU treatment. Confocal laser scanning microscopy (CLSM) and scanning electron microscopy (SEM) observations revealed that the particle size of the emulsion gels was decreased significantly by HIU treatment. The emulsion gel structure became more uniform and denser, which was conducive to storage stability. In addition, according to the low field nuclear magnetic resonance (LF-NMR) analysis, HIU treatment had no obvious impact on the content of bound water as the power increased to 450 W, while the content of free water decreased gradually and became immobilized water, which indicated that the water holding capacity of the emulsion gels was enhanced. Compared with untreated emulsion gel, differential scanning calorimetry (DSC) analysis showed that the denaturation temperature reached 131.9 ℃ from 128.2 ℃ when treated at 450 W. The chemical stability and bioaccessibility of β-carotene in the emulsion gels were improved significantly after HIU treatment during simulated *in vitro* digestion.

1. Introduction

An emulsion gel is a gel-like solid material with a spatial network structure formed through a certain induction method on the basis of the emulsion. It is characterized by emulsified oil droplets in the gel network [1,2]. Recently, emulsion gel has attracted increasing attention because it can be used in meat products instead of animal fat. Otherwise, emulsion gel can also be used as a delivery system for some biologically active substances, such as vitamins, β-carotene, and curcumin [3-5]. After being solidified by the spatial structure, these active substances can be protected by the emulsion gel, and the chemical stability can be improved significantly [6].

It is worth noting that emulsion gels, which are prepared with protein or polysaccharide alone, usually have some limitations in practical applications, such as poor emulsification and thermal stability. This has shifted the research focus gradually to emulsion gels stabilized by multiple substances [7,8]. This can not only enhance the emulsification of individual substances but also help to resist environmental changes such as extreme pH, ionic strength and heat treatment and improve the stability of emulsion gels [9,10]. Soybean protein isolate (SPI) is a plant protein resource with a wide range of sources. When SPI is used as an emulsifier, it is often affected by its natural structure, processing and storage, resulting in a decline in its functional properties. Pectin is commonly used as a thickener and gelling agent in the food industry. Therefore, SPI and pectin were selected as raw materials to prepare emulsion gels in this study. In addition, β-carotene has strong antioxidant activity, but it is extremely sensitive to light and heat, which may lead to the loss of its biological activity. An emulsion gel delivery system can effectively protect β-carotene from degradation.

Moreover, an emulsion gel with a denser and more uniform network structure can be obtained through appropriate treatment and modification, thus affecting the stability and release rate of the embedded active substances. High intensity ultrasound (HIU) treatment is a new type of physical modification method that has the advantages of high energy, high safety, environmental friendliness and strong penetrating power [11,12]. HIU emulsification is mainly provoked by the cavitation

* Corresponding author.
E-mail addresses: dyyu2000@126.com (D. Yu), pmz_1223.student@sina.com (M. Pan).

https://doi.org/10.1016/j.ultsonch.2021.105756
Received 13 August 2021; Received in revised form 4 September 2021; Accepted 13 September 2021
Available online 16 September 2021

effect. The high temperature and high pressure generated by instantaneous bursts of cavitation bubbles will produce physical, chemical and thermal effects on the materials in solution. Under these conditions, the properties of emulsions can be affected by modification methods [13,14]. Among them, the physical effects are mainly produced by physical forces, including shear force, high pressure, shock waves and microjets [15,16]. The chemical effects mainly refer to the free radicals produced by ultrasound, which can oxidize any substance in the emulsion or react with each other to form H_2O_2. In addition, amino acids such as Trp, His and Cys in proteins are easily oxidized, and free radicals and H_2O_2 can also attack polyunsaturated fatty acids in oil [17,18]. Finally, thermal effects may affect the unfolding of proteins, the properties of polysaccharides, and the oxidation of lipids. The increase in local temperature in the emulsion and the instantaneous high temperature may have a great impact on the properties of the emulsion [13].

Hence, HIU technology was used to process SPI and pectin emulsions, and then the emulsion gel system was prepared by thermal induction. The effects of HIU treatment on the structure, gel properties and stability of the emulsion gel were studied. In addition, *in vitro* digestion simulation experiments were conducted on emulsion gels containing β-carotene to explore the influence of HIU treatment on the stability of β-carotene during digestion. This research provides a theoretical basis for the development of a good emulsification system for the delivery of biologically active substances.

2. Materials and methods

2.1. Materials

SPI was prepared in our laboratory. Defatted soybean powder was mixed with deionized water, and the pH was adjusted to 8.0. The dispersion was subjected to protein extraction with magnetic stirring for 2.5 h and then centrifuged at 10000 × *g* and 4 °C for 30 min. The supernatant was adjusted to pH 4.5 and centrifuged at 10000 × *g* for 30 min. The precipitate was washed twice with deionized water and then neutralized to pH 7.0. The neutral solution was frozen and subsequently freeze-dried for further use. The protein content of SPI was 90.62% ± 0.84% by the Kjeldahl method. High methoxy methyl ester pectin (derived from citrus, degree of esterification (DE) > 50%) and β-carotene were purchased from Yuanye Biotechnology Co., Ltd. (Shanghai, China). First-grade soybean oil was obtained from Jiusan Huikang Food Co., Ltd. (Harbin, Heilongjiang, China). All other chemical agents were of analytical grade.

2.2. Preparation of emulsion

SPI (final concentration 7%) and pectin (final concentration 3%) were dispersed in sodium phosphate buffer (PBS, 0.01 M, pH 7.0). The solution was continuously stirred for 3 h at room temperature to ensure a complete reaction of the SPI and pectin. Next, the solution was mixed with 6% (v/v) soybean oil (with/without 3 wt% β-carotene) and homogenized (Ultra-Turrax T18, Angni Co., Shanghai, China) at 20000 rpm for 5 min. Incidentally, soybean oil containing β-carotene was obtained by heating at 140 °C for 2 min with continuous stirring.

2.3. Preparation of emulsion gel

The prepared emulsions were placed in a large beaker with ice to keep the temperature below 20 ℃, and a titanium probe with a diameter of 6 mm was immersed in the emulsions at a depth of 1 cm from the bottom, followed by treatment with HIU at different output powers (0, 150, 300, 450 and 600 W) at 20 kHz for 15 min (pulse duration of 4 s on and 2 s off) using an ultrasonic generator (Scientz Biotechnology Co., Ltd., Ningbo, China), while ensuring that the probe position in each group of samples was at the same depth from the bottom. Finally, the emulsions were heated for 30 min at 80 °C, allowed to coagulate in a water bath, and then cooled in an ice water bath immediately. After coagulation, the emulsion gels were stored at 4 °C until further analysis. The emulsion gels were prepared according to the method outlined above with β-carotene dissolved in soybean oil and used for *in vitro* digestion simulation.

2.4. Fourier transform infrared spectroscopy (FTIR)

FTIR was used to characterize the interaction between SPI and pectin in emulsion gels by KBr tableting [19]. The freeze-dried emulsion gels were mixed with KBr at a ratio of 1:100 and ground evenly. Then, the samples were pressed and measured from 4000 to 500 cm^{-1}.

2.5. X-ray diffraction (XRD)

The XRD data of emulsion gels treated with different ultrasound powers were obtained using an X-ray diffractometer (D/MAX 2500 V, Rigaku Corporation, Japan) at 40 kV. The samples were laid flat in the circular hole on the test piece and scanned from 5° to 150° (2θ) [20]. Then, the degree of crystallinity was calculated.

2.6. Confocal laser scanning microscopy (CLSM)

The distribution and size of the emulsion gels were evaluated using CLSM (Leica Microsystems, Heidelberg GmbH, Germany). First, Nile blue and Nile red were dissolved in isopropanol to prepare 1% and 0.1% staining solutions, respectively, and then mixed uniformly and filtered. Next, 25 μL Nile blue solution and 20 μL Nile red solution were added to 0.5 mL of emulsion treated with different ultrasound powers and allowed to stain for 30 min. The gelation process was carried out in accordance with the method mentioned above. Confocal images were obtained with a 100X magnification lens [21].

2.7. Scanning electron microscopy (SEM)

The microstructure of the emulsion gels was observed by SEM (S-3400 N, Hitachi, Tokyo, Japan) according to the method of Wang et al. [22]. The emulsion gels were cut into small pieces and immersed in 2.5% glutaraldehyde for 24 h, rinsed with PBS (0.1 M, pH 7.2) three times and dehydrated with 50%, 70%, 90% and 100% ethanol. After dehydration, the samples were freeze-dried and sputter-coated for microscopic observation.

2.8. Water holding capacity (WHC)

The WHC of emulsion gels was measured using a method described by Bi et al. [23]. The emulsion gels were weighed and centrifuged at 10,000 × *g* for 20 min at 4 °C. The calculation formula for WHC was expressed as:

$$\mathrm{WHC} = \frac{W_1 - W_2}{W_1} \times 100\%$$

where W_1 is the mass of the emulsion gel before centrifugation, and W_2 is the mass of the water removed after centrifugation.

2.9. Gel strength

A texture analyzer (Stable Micro Systems Co. Ltd., Surrey, UK) was used to perform a puncture test on emulsion gels treated with different ultrasound powers at room temperature to measure the breaking strength [24].

2.10. Low field nuclear magnetic resonance (LF-NMR)

LF-NMR was used to determine the water distribution in the

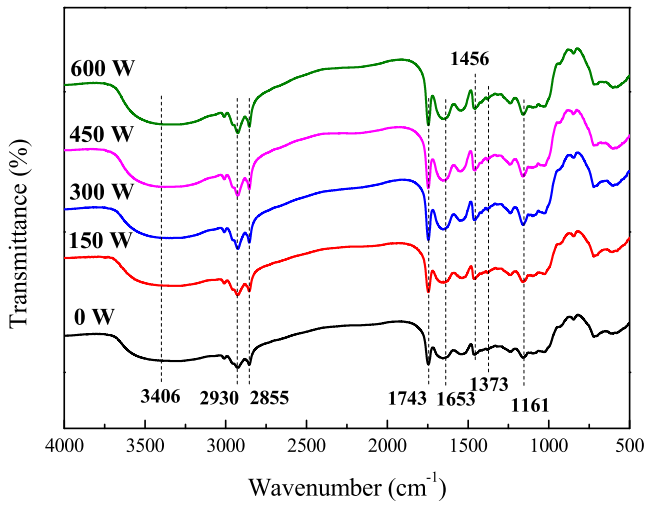

Fig. 1. FTIR analysis of emulsion gels treated with different ultrasound powers.

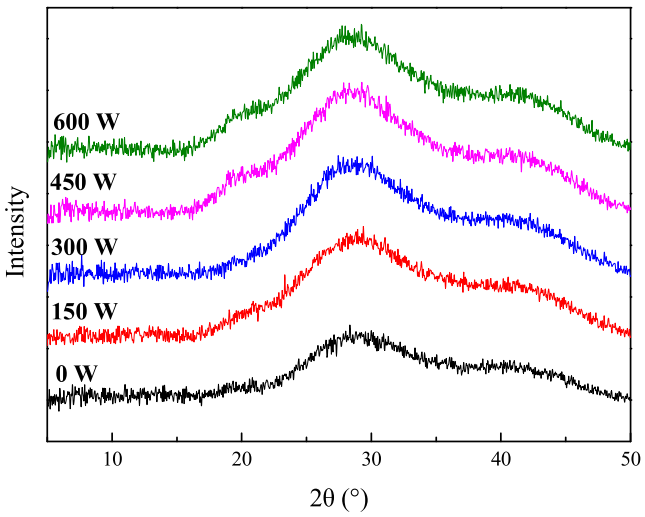

Fig. 2. XRD analysis of emulsion gels treated with different ultrasound powers.

emulsion gels treated with different ultrasound powers according to a method outlined by Zhang et al. [25]. The emulsion gels were placed in a cylindrical glass tube (15 mm diameter) and inserted into the NMR probe. The transverse relaxation time (T_2) was measured with an LF-NMR analyzer (Bruker Optik GmbH, Ettlingen, Germany).

2.11. Differential scanning calorimetry (DSC)

A DSC 250 (TA instrument, USA) was used to measure the thermal behavior of the emulsion gels. Two milligrams of emulsion gel was placed in an aluminum disc and sealed with an aluminum cover. The initial scanning temperature was set at 20 °C and increased to 150 °C at a heating rate of 5 °C/min.

2.12. In vitro digestion

2.12.1. Simulated gastrointestinal tract digestion

Gastric stage: Emulsion gel samples with β-carotene treated by different ultrasound powers were dispersed in 10 mL of distilled water, which was adjusted to pH 6.0, and mixed with simulated gastric fluid containing 3.2 mg/mL pepsin at a ratio of 1:1 (v/v) in conical flasks. Subsequently, the pH of the samples was adjusted to 2.5 with 1 M HCl solution, and then gastric digestion was simulated at 37 °C with continuous shaking for 1 h.

Intestinal stage: The pH of the samples after the gastric digestion stage was adjusted to 7.5 with a 1 M NaOH solution to inactivate pepsin. A 10 mL sample was mixed with simulated intestinal fluid containing 20 mg/mL bile salt, 10 mg/mL lipase, and 10 mg/mL pancreatin at a ratio of 1:1 (v/v), and the pH was adjusted to 7.5 again. The samples were kept at 37 °C for 2 h to simulate intestinal digestion.

2.12.2. Bioaccessibility and chemical stability of β-carotene

At the end of the *in vitro* digestion simulation, the samples were centrifuged at 10,000 × g for 30 min to collect the intermediate micellar phase. β-Carotene was extracted with a mixed solvent of n-hexane, acetone and ethanol (v/v, 2:1:1). The absorbance at 450 nm was recorded to determine the content of β-carotene. The equations for calculating the bioaccessibility and chemical stability of β-carotene were as follows [26]:

$$\text{Bioaccessibility} = \frac{C_M}{C_D} \times 100\%$$

$$\text{Chemical stability} = \frac{C_D}{C_G} \times 100\%$$

where C_M is the concentration of β-carotene in the micelle phase, C_D is the concentration of β-carotene in the sample after intestinal digestion, and C_G is the concentration of β-carotene in the emulsion gel.

2.13. Statistical analysis

All test indicators in this study were repeated at least three times. The average and standard error were calculated and analyzed, and the data were recorded by Excel. Origin 8.5 was used for drawing, SPSS 22.0 was used for one-way analysis of variance (ANOVA), and Duncan's test ($p < 0.05$) was used to verify the significance of the data differences.

3. Results and discussion

3.1. FTIR analysis

The FTIR spectroscopy results of the emulsion gels treated with different ultrasound powers are shown in Fig. 1. The broad peak at 3406 cm^{-1} was attributed to the stretching vibration of OH, and asymmetric and symmetric stretching vibrations of CH were observed at 2930 cm^{-1} and 2855 cm^{-1} [27]. With increasing HIU power, the stretching vibration peaks of CH increased, which may be due to the enhanced hydrogen bonding between the methylene group of pectin and the hydroxyl group of SPI [28]. The bands in the region of 1200–1800 cm^{-1} belonged to the main functional groups present in pectin [29]. For example, the band at 1743 cm^{-1} was attributable to the C=O stretching of the methyl ester (usually used to detect the degree of esterification of pectin). The peaks at 1653 cm^{-1} and 1373 cm^{-1} were related to the C=O asymmetric and symmetric stretching of the COO^{-} group of polygalacturonic acid in pectin, respectively. The peak at 1456 cm^{-1} was due to the bending vibration of CH_2, and the peak at 1161 cm^{-1} was the stretching vibration of C–O–C. In addition, with increasing HIU processing power, the peak intensity at 1161 cm^{-1} increased, which was related to the extension of C–O–C. It can be seen from the spectrogram that the interaction of the internal groups in the emulsion gels was affected by HIU treatment; however, the basic gel structure was not destroyed. This may be attributed to the shear force and turbulence caused by HIU, which played an important role in the structure of SPI and pectin. Moreover, the heat and oxidation produced by the cavitation effect also affected the structure of SPI and pectin. Furthermore, the peak intensity of the 3406 cm^{-1} region corresponding to hydrogen bonds increased, which indicates that the interaction between SPI and pectin was enhanced due to HIU treatment.

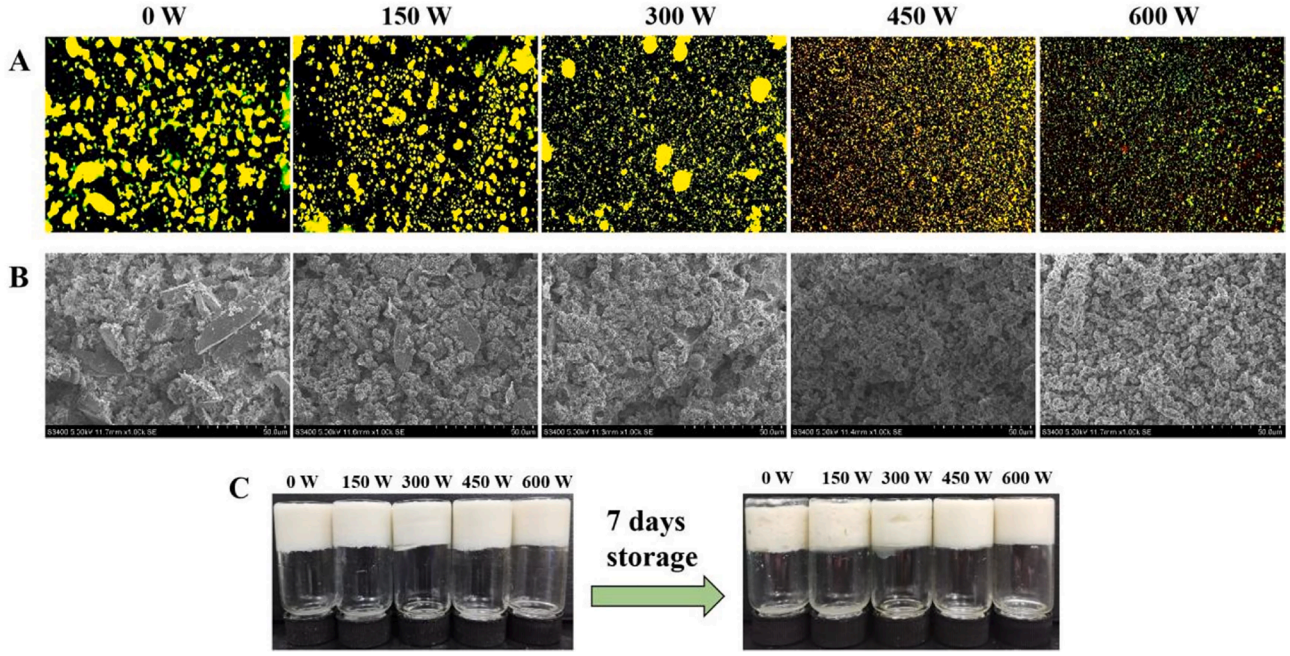

Fig. 3. CLSM micrographs (A), SEM micrographs (B) and storage stability (C) of emulsion gels treated with different ultrasound powers.

3.2. XRD analysis

Fig. 2 shows the XRD spectra of emulsion gels treated with different ultrasound powers. All samples exhibited a clearly broad diffraction peak at approximately $2\theta = 29°$. Compared with the untreated emulsion gel, the crystallinity of the sample with an HIU power of 450 W increased from 22.7% to 26.4%. Moreover, the diffraction peaks of HIU-treated emulsion gels moved to higher angles with respect to the XRD pattern of the untreated emulsion gel. These results indicated that the crystal size of the emulsion gel decreased after HIU treatment [30,31]. This is probably because the regular arrangement of protein and pectin molecules was destroyed as a result of HIU treatment. This reduced the overall rigidity and therefore caused the crystal size of the emulsion gels to decrease after heat induction.

3.3. Microstructure analysis

The micrographs of emulsion gels were observed by CLSM. Fig. 3A shows that the droplet size of the emulsion gel gradually decreased when treated at low HIU powers of 150 and 300 W, but there was still obvious aggregation. However, when treated at 450 and 600 W, the aggregation was significantly improved, and the emulsion gels were composed of homogeneous small particles. This may be due to the exposure of more hydrophobic groups in SPI after being processed by HIU [18,32]. This enhanced the interaction between the unadsorbed/adsorbed SPI and pectin on the surface of oil droplets, as well as the interaction between free proteins and interfacial proteins, to better encapsulate the oil phase, which is conducive to the gelation of emulsions. Furthermore, the uniformity of the emulsion gel was improved by high HIU treatment power. Smaller droplets were coated with SPI and pectin, which had larger surface areas and aggregated through stronger physical and chemical interactions, resulting in a denser emulsion gel structure [33].

The SEM images of emulsion gels are shown in Fig. 3B. The spheroidal particles formed by the oil droplets wrapped by SPI and pectin and the SPI and pectin that were not adsorbed into the oil–water interface were the main structural units, which constructed a complete emulsion gel network [34]. The untreated emulsion gel had a coarser structure and larger particle size, which was consistent with that observed by CLSM. Moreover, a small amount of SPI and pectin was apparently not adsorbed onto the interface, and the gel structures composed of these SPIs and pectin and spherical particles were relatively loose, which may lead to a decrease in the ability of the emulsion gel to bind water. With the increasing power of HIU treatment, the interaction between SPI and pectin and the oil droplets increased, resulting in the emulsion gel becoming more uniform and denser [35], and there was no obvious aggregation of SPI and pectin on the surface of the emulsion gel when the HIU power was greater than 450 W.

In addition, HIU treatment significantly improved the storage stability of the emulsion gel. Fig. 3C shows that after storage at room temperature for 7 days, part of the water was separated from the emulsion gel without ultrasound treatment, and the gel structure became loose. However, this situation was improved with increasing ultrasound power. When the emulsion gels were treated with HIU at 450 W and 600 W, the initial gel structure was maintained after storage, and only a minute quantity of water precipitated.

Table 1
Gel strength and WHC of emulsion gels treated with different ultrasound powers.

Ultrasound power (W)	Gel strength(N)	WHC(%)
0	0.2732 ± 0.0260^{e}	92.56 ± 0.09^{e}
150	0.3317 ± 0.0207^{d}	94.49 ± 0.03^{d}
300	0.4472 ± 0.0252^{bc}	96.87 ± 0.06^{c}
450	0.5283 ± 0.0184^{a}	98.82 ± 0.08^{a}
600	0.4758 ± 0.0173^{b}	97.25 ± 0.07^{b}

Note: The values with different superscript letters (a-e) within a column are significantly different ($p < 0.05$).

3.4. Gel strength and WHC analysis

Table 1 shows the strength of the emulsion gel, and the gel strength after HIU treatment at different powers showed a trend of first increasing and then decreasing with increasing ultrasound power. This may be attributed to the cavitation effect caused by HIU, which fully unfolded the structure of SPI and pectin. The interaction between SPI, pectin and oil droplets was enhanced by hydrogen bonding, Van der Waals forces and hydrophobic interactions. This is beneficial to the formation of a more compact and uniform emulsion gel in a three-

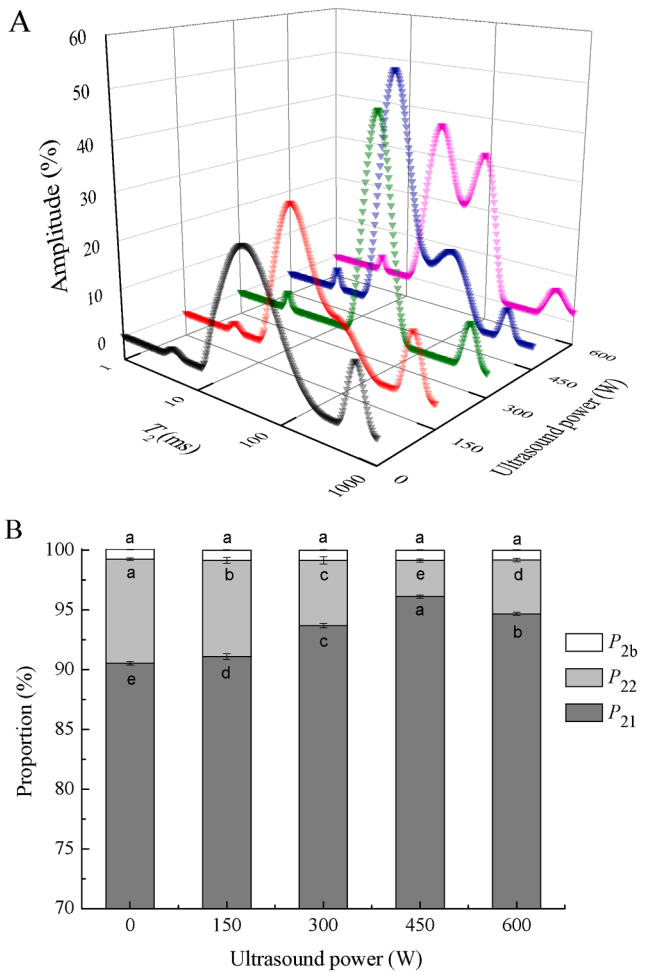

Fig. 4. Distribution of the LF-NMR T_2 relaxation times (A) and T_2 peak ratio (B) of emulsion gels treated with different ultrasound powers.

dimensional network structure, resulting in higher gel strength [36]. However, the gel strength decreased when the power of HIU treatment increased to 600 W, probably due to excessive ultrasound treatment. This resulted in aggregation of protein particles and formation of insoluble aggregates; thus, the interaction between the emulsion gel and water was weakened. In addition, the structure of these insoluble aggregates was more compact than a three-dimensional network structure. In this case, the emulsion gel was more likely to break when an external stress was applied. The macroscopic performance was the decrease in gel strength, which was consistent with that observed by SEM.

WHC, which is one of the important characteristics of evaluating the structure of the emulsion gel, indicates the ability of emulsion gel systems to fix water [37]. According to Table 1, the WHC of emulsion gels increased significantly ($p < 0.05$) after HIU treatment compared with that of untreated emulsion gel (92.56% ± 0.09%). It may be that the particle size of emulsion gel was decreased under the action of ultrasound and that the interface area between oil and water in the emulsion gel increased. This resulted in a more stable gel system formed, which can effectively combine water into the emulsion gel matrix. Therefore, the WHC and strength of the emulsion gel increased. On the other hand, the structure of the emulsion gel became loose due to the insoluble aggregates produced by excessive ultrasound at 600 W, and thus the WHC was weakened. Overall, these results further proved that HIU could effectively make the emulsion gel more uniform and denser, which also contributed to the enhancement of gel strength and WHC.

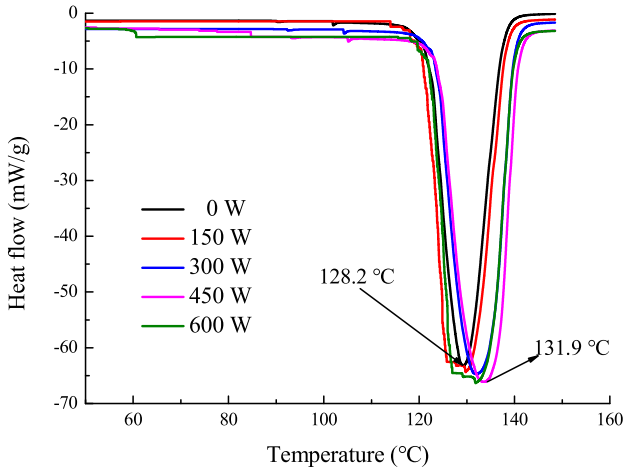

Fig. 5. DSC curves of emulsion gels treated with different ultrasound powers.

3.5. LF-NMR analysis

LF-NMR has been widely used to study proton mobility in protein/polysaccharide gel systems, as it can intuitively reflect the water distribution in emulsion gels [38]. Fig. 4A shows the relaxation time (T_2) of the emulsion gels treated with different ultrasound powers. In this study, three peaks were observed, where T_{2b} (1–10 ms) reflected the bound water in the gel network, T_{21} (10–600 ms) represented immobilized water, and T_{22} (600–1000 ms) corresponded to free water, indicating the movement of water in the emulsion gel. P_{2b}, P_{21}, and P_{22} were the corresponding area fractions, as shown in Fig. 4B. HIU treatment had no significant effect on the bound water in the emulsion gel. However, the immobilized water and free water began to move toward the direction of the bound water as the ultrasound power increased. This indicated that the HIU treatment enhanced the ability of the emulsion gel to bind water. It is worth noting that the area fraction of P_{22} was the smallest when the HIU power was 450 W, indicating that the free water was converted to immobilized water, which helped to enhance the WHC of the emulsion gel (Table 1). Moreover, the particle size of SPI and pectin were effectively reduced by the appropriate ultrasound power, which is conducive to the emulsion gel network capturing more water [39].

3.6. DSC analysis

The effect of HIU treatment on the thermal properties of emulsion gels was studied by DSC. As shown in Fig. 5, all samples exhibited an obvious absorption peak between 125 and 132 ℃ of the thermal characteristic curves, which may be related to the evaporation of the bound water and represented the denaturation temperature of the emulsion gel, indicating that all the emulsion gels had good thermal stability [40]. The denaturation temperature of the emulsion gel without HIU treatment was 128.2 °C. The absorption peak began to gradually shift to the right with increasing HIU treatment power; that is, the denaturation temperature was increased. The emulsion gel reached the highest denaturation temperature (131.9 ℃) when treated with HIU at 450 W. This may be due to the loose structure of the emulsion gel when treated at low HIU powers of 150 and 300 W, which led to weak resistance to heat. The interaction between SPI and pectin was strengthened after 450 W ultrasound treatment, and the interfacial area of oil–water was increased; thus, a more stable emulsion gel structure with a smaller particle size was formed (Fig. 3 AB). In other words, the complete denaturation of the emulsion gel required more heat absorption due to the HIU treatment, which led to the improvement of the thermal stability. In addition, the absorption peak shifted slightly to the left when treated with HIU at 600 W. These results were consistent with the above

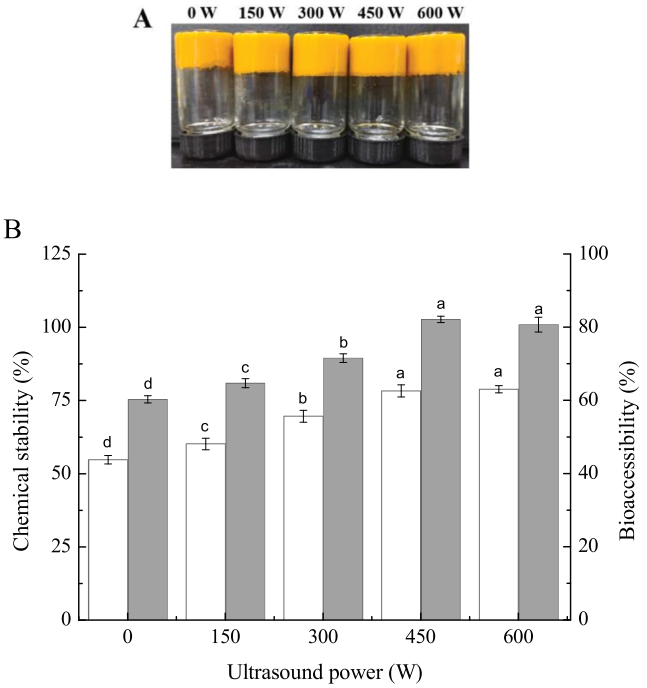

Fig. 6. Photographs of β-carotene-containing emulsion gels treated with different ultrasound powers (A) and the chemical stability and bioaccessibility of emulsion gels after *in vitro* digestion (B).

analysis, which indicated that excessive ultrasound treatment had an adverse effect on the structural properties and stability of emulsion gels.

3.7. *In vitro digestion*

β-Carotene has strong antioxidant activity, but its biological activity is easily lost due to its extreme sensitivity to light and heat. Studies have shown that β-carotene can be well protected from degradation by delivery systems such as emulsions, gels, and nanoparticles [41]. For this purpose, *in vitro* digestion experiments were carried out to investigate the effect of HIU treatment at different powers on the chemical stability and bioaccessibility of β-carotene in the emulsion gel. Fig. 6A shows pictures of β-carotene-containing emulsion gels treated with HIU at different powers. The chemical stability and bioaccessibility of β-carotene in the emulsion gel after *in vitro* digestion are shown in Fig. 6B. The bioaccessibility of β-carotene was significantly improved by HIU treatment. This may be attributed to the reduction of oil droplet aggregation during the digestion of the emulsion gel network processed by HIU treatment, resulting in the probability of lipase approaching the surface of oil droplets being promoted. Therefore, the content of β-carotene released into the micelles increased [42]. Furthermore, the chemical stability of β-carotene after *in vitro* digestion was 78.3 ± 2.0% when treated with HIU at 450 W, which was significantly higher than that of the emulsion gel without ultrasound treatment (54.8% ± 1.5%) ($p < 0.05$), indicating that the degradation of β-carotene encapsulated in the emulsion gel was reduced [43]. In summary, the network structure of the emulsion gel was more stable after HIU treatment, and the diffusion of substances such as oxygen and free radicals to the surface of oil droplets slowed down; therefore, the degradation of β-carotene in the gastrointestinal tract was effectively delayed.

Based on the results outlined above, the effect of HIU treatment on the formation mechanism of emulsion gels is shown in Fig. 7. Cavitation caused by HIU mainly affected the structure and stability of the emulsion gels through physical, chemical and thermal effects. First, the large droplets in the emulsion were directly broken into small particles due to physical forces during the HIU process. The shear force and high pressure generated by the instantaneous bursting of cavitation bubbles reduced the particle size of SPI and pectin and caused the molecular structure to unfold, which was conducive to the enhancement of intermolecular interactions (Fig. 1). Therefore, the interfacial tension of the emulsion was effectively reduced, and an emulsion gel with a smaller particle size and a more uniform gel network was formed after heating (Fig. 3AB). Furthermore, free radicals and high temperature generated by cavitation resulted in a certain extent of SPI and pectin oxidation, which also promoted the unfolding of molecular structure, improving storage and thermal stability of the emulsion gel (Fig. 3C and Fig. 5). However, excessive ultrasound treatment gave rise to more free radicals and heat when treated at 600 W. The H_2O_2 formed by the mutual reaction of free radicals and the high local temperature of emulsion caused

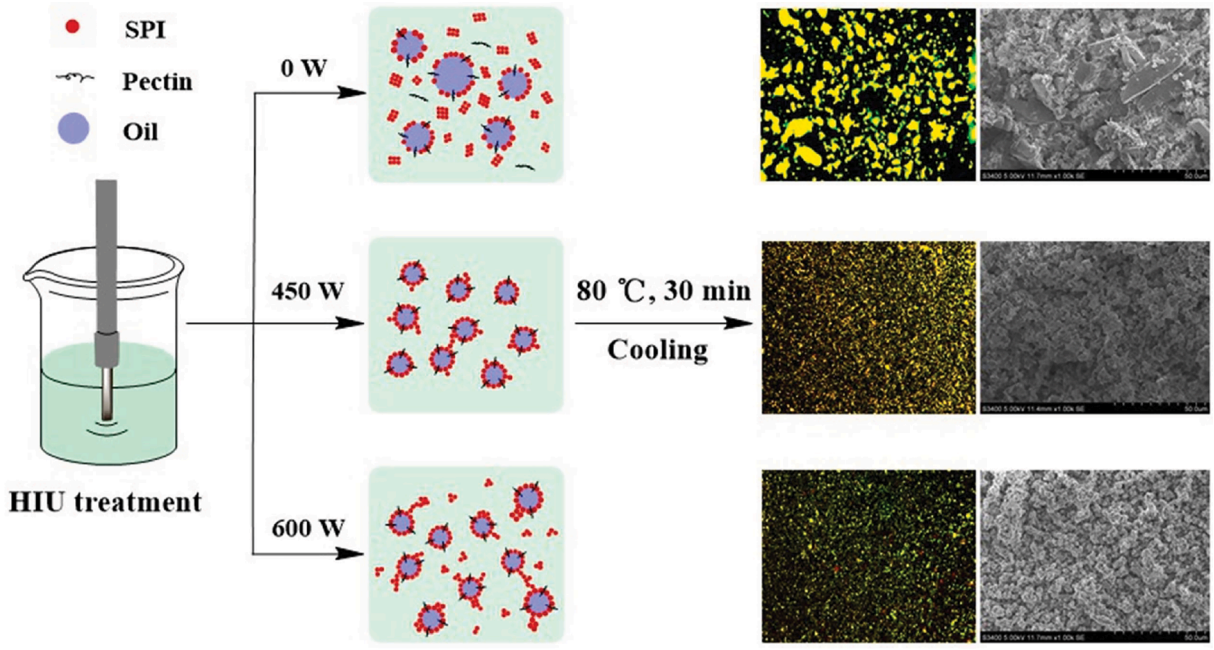

Fig. 7. Schematic diagram of improving the stability of emulsion gel by HIU.

by the burst of cavitation bubbles led to the protein being oxidized and aggregated into insoluble aggregates, which adversely affected the stability of the emulsion gel.

4. Conclusions

The influence of HIU at various powers on the structure, gel properties and stability of SPI and pectin emulsion gels was evaluated. The interaction between SPI and pectin was enhanced, and the emulsion gels had smaller crystal sizes after HIU treatment. Microstructure, gel strength and DSC analysis showed that the emulsion gel had the most compact and densest network and the best thermal stability when treated at 450 W. LF-NMR results revealed that the WHC of emulsion gels was improved by HIU treatment. The results of *in vitro* simulated digestion showed that the chemical stability and bioaccessibility of β-carotene in emulsion gels were increased significantly after treatment at proper ultrasound power. Overall, this research provides a theoretical basis for the construction of SPI and pectin emulsion gel systems, which is conducive to the development of functional food delivery systems loaded with biologically active substances.

CRediT authorship contribution statement

Xin Zhang: Methodology, Investigation, Writing – original draft. **Xing Chen:** Investigation, Validation, Data curation. **Yuhang Gong:** Data curation, Visualization. **Ziyue Li:** Conceptualization, Formal analysis. **Yanfei Guo:** Data curation. **Dianyu Yu:** Conceptualization, Methodology, Writing - review & editing. **Mingzhe Pan:** Supervision, Funding acquisition.

Declaration of Competing Interest

The authors declare that they have no known competing financial interests or personal relationships that could have appeared to influence the work reported in this paper.

Acknowledgements

This work was supported by a grant from the Hundred Thousand and Ten thousand Project of China: Integration and demonstration of key technologies for soybean bio-based oil and protein products (No: 2020ZX08B01).

References:

[1] D. Lin, A.L. Kelly, S. Miao, Preparation, structure-property relationships and applications of different emulsion gels: Bulk emulsion gels, emulsion gel particles, and fluid emulsion gels, Trends Food Sci. Technol. 102 (2020) 123–137, https://doi.org/10.1016/j.tifs.2020.05.024.

[2] T. Farjami, A. Madadlou, An overview on preparation of emulsion-filled gels and emulsion particulate gels, Trends Food Sci. Technol. 86 (2019) 85–94, https://doi.org/10.1016/j.tifs.2019.02.043.

[3] Z. Shi, Z. Shi, M. Wu, Y. Shen, G. Li, T. Ma, Fabrication of emulsion gel based on polymer sanxan and its potential as a sustained-release delivery system for β-carotene, Int. J. Biol. Macromol. 164 (2020) 597–605, https://doi.org/10.1016/j.ijbiomac.2020.07.177.

[4] J. Su, Q. Guo, Y. Chen, W. Dong, L. Mao, Y. Gao, F. Yuan, Characterization and formation mechanism of lutein pickering emulsion gels stabilized by β-lactoglobulin-gum arabic composite colloidal nanoparticles, Food Hydrocolloids 98 (2020) 105276, https://doi.org/10.1016/j.foodhyd.2019.105276.

[5] I.M. Geremias-Andrade, N.P.D.B.G. Souki, I.C.F. Moraes, S.C. Pinho, Rheological and mechanical characterization of curcumin-loaded emulsion-filled gels produced with whey protein isolate and xanthan gum, LWT. 86 (2017) 166–173, https://doi.org/10.1016/j.lwt.2017.07.063.

[6] D.J. Mcclements, Recent progress in hydrogel delivery systems for improving nutraceutical bioavailability, Food Hydrocolloids 68 (2017) 238–245, https://doi.org/10.1016/j.foodhyd.2016.05.037.

[7] B. Chen, D.J. McClements, D.A. Gray, E.A. Decker, Stabilization of Soybean Oil Bodies by Enzyme (Laccase) Cross-Linking of Adsorbed Beet Pectin Coatings, J. Agric. Food. Chem. 58 (16) (2010) 9259–9265, https://doi.org/10.1021/jf102082u.

[8] B. Zeeb, M. Gibis, L. Fischer, J. Weiss, Crosslinking of interfacial layers in multilayered oil-in-water emulsions using laccase: Characterization and pH-stability, Food Hydrocolloids 27 (1) (2012) 126–136, https://doi.org/10.1016/j.foodhyd.2011.08.005.

[9] L. Dai, C. Sun, Y. Wei, L. Mao, Y. Gao, Characterization of Pickering emulsion gels stabilized by zein/gum arabic complex colloidal nanoparticles, Food Hydrocolloids 74 (2018) 239–248, https://doi.org/10.1016/j.foodhyd.2017.07.040.

[10] T.C. Brito-Oliveira, M. Bispo, I.C.F. Moraes, O.H. Campanella, S.C. Pinho, Stability of curcumin encapsulated in solid lipid microparticles incorporated in cold-set emulsion filled gels of soy protein isolate and xanthan gum, Food Res. Int. 102 (2017) 759–767, https://doi.org/10.1016/j.foodres.2017.09.071.

[11] A. Córdova, C. Astudillo-Castro, R. Ruby-Figueroa, P. Valencia, C. Soto, Recent advances and perspectives of ultrasound assisted membrane food processing, Food Res. Int. 133 (2020) 109163, https://doi.org/10.1016/j.foodres.2020.109163.

[12] O.A. Higuera-Barraza, C.L. Del Toro-Sanchez, S. Ruiz-Cruz, E. Márquez-Ríos, Effects of high-energy ultrasound on the functional properties of proteins, Ultrason. Sonochem. 31 (2016) 558–562, https://doi.org/10.1016/j.ultsonch.2016.02.007.

[13] L. Zhou, J. Zhang, L. Xing, W. Zhang, Applications and effects of ultrasound assisted emulsification in the production of food emulsions: A review, Trends Food Sci. Technol. 110 (2021) 493–512, https://doi.org/10.1016/j.tifs.2021.02.008.

[14] C. Ozuna, I. Paniagua-Martínez, E. Castaño-Tostado, L. Ozimek, S.L. Amaya-Llano, Innovative applications of high-intensity ultrasound in the development of functional food ingredients: Production of protein hydrolysates and bioactive peptides, Food Res. Int. 77 (2015) 685–696, https://doi.org/10.1016/j.foodres.2015.10.015.

[15] S. Mohamadi, J. Abdolalizadeh, S. Zeinali, Ultrasonic/sonochemical synthesis and evaluation of nanostructured oil in water emulsions for topical delivery of protein drugs, Ultrason. Sonochem. 55 (2019) 86–95, https://doi.org/10.1016/j.ultsonch.2019.03.018.

[16] A.C. Soria, M. Villamiel, Effect of ultrasound on the technological properties and bioactivity of food: a review, Trends Food Sci. Technol. 21 (7) (2010) 323–331, https://doi.org/10.1016/j.tifs.2010.04.003.

[17] M. Munir, M. Nadeem, T.M. Qureshi, T.S.H. Leong, C.J. Gamlath, G.J.O. Martin, M. Ashokkumar, Effects of high pressure, microwave and ultrasound processing on proteins and enzyme activity in dairy systems — A review, Innovative Food Sci. Emerg. Technol. 57 (2019) 102192, https://doi.org/10.1016/j.ifset.2019.102192.

[18] A. Taha, T. Hu, Z. Zhang, A.M. Bakry, I. Khalifa, S. Pan, H. Hu, Effect of different oils and ultrasound emulsification conditions on the physicochemical properties of emulsions stabilized by soy protein isolate, Ultrason. Sonochem. 49 (2018) 283–293, https://doi.org/10.1016/j.ultsonch.2018.08.020.

[19] K.M. Albano, V.R. Nicoletti, Ultrasound impact on whey protein concentrate-pectin complexes and in the O/W emulsions with low oil soybean content stabilization, Ultrason. Sonochem. 41 (2018) 562–571, https://doi.org/10.1016/j.ultsonch.2017.10.018.

[20] Y.-R. Wang, B. Zhang, J.-L. Fan, Q. Yang, H.-Q. Chen, Effects of sodium tripolyphosphate modification on the structural, functional, and rheological properties of rice glutelin, Food Chem. 281 (2019) 18–27, https://doi.org/10.1016/j.foodchem.2018.12.085.

[21] P. Lv, D.i. Wang, Y. Chen, S. Zhu, J. Zhang, L. Mao, Y. Gao, F. Yuan, Pickering emulsion gels stabilized by novel complex particles of high-pressure-induced WPI gel and chitosan: Fabrication, characterization and encapsulation, Food Hydrocolloids 108 (2020) 105992, https://doi.org/10.1016/j.foodhyd.2020.105992.

[22] X. Wang, Z. He, M. Zeng, F. Qin, B. Adhikari, J. Chen, Effects of the size and content of protein aggregates on the rheological and structural properties of soy protein isolate emulsion gels induced by $CaSO_4$, Food Chem. 221 (2017) 130–138, https://doi.org/10.1016/j.foodchem.2016.10.019.

[23] C.-H. Bi, P.-L. Wang, D.-y. Sun, Z.-M. Yan, Y.i. Liu, Z.-G. Huang, F. Gao, Effect of high-pressure homogenization on gelling and rheological properties of soybean protein isolate emulsion gel, J. Food Eng. 277 (2020) 109923, https://doi.org/10.1016/j.jfoodeng.2020.109923.

[24] Y. Lv, L. Chen, H. Wu, X. Xu, G. Zhou, B. Zhu, X. Feng, (-)-Epigallocatechin-3-gallate-mediated formation of myofibrillar protein emulsion gels under malondialdehyde-induced oxidative stress, Food Chem. 285 (2019) 139–146, https://doi.org/10.1016/j.foodchem.2019.01.147.

[25] C. Zhang, X.-a. Li, H. Wang, X. Xia, B. Kong, Ultrasound-assisted immersion freezing reduces the structure and gel property deterioration of myofibrillar protein from chicken breast, Ultrason. Sonochem. 67 (2020) 105137, https://doi.org/10.1016/j.ultsonch.2020.105137.

[26] C. Soukoulis, M. Tsevdou, C.M. Andre, S. Cambier, L. Yonekura, P.S. Taoukis, L. Hoffmann, Modulation of chemical stability and in vitro bioaccessibility of beta-carotene loaded in kappa-carrageenan oil-in-gel emulsions, Food Chem. 220 (2017) 208–218, https://doi.org/10.1016/j.foodchem.2016.09.175.

[27] C. Kyomugasho, S. Christiaens, A. Shpigelman, A.M. Van Loey, M.E. Hendrickx, FT-IR spectroscopy, a reliable method for routine analysis of the degree of methylesterification of pectin in different fruit- and vegetable-based matrices, Food Chem. 176 (2015) 82–90, https://doi.org/10.1016/j.foodchem.2014.12.033.

[28] N. Bhargava, R.S. Mor, K. Kumar, V.S. Sharanagat, Advances in application of ultrasound in food processing: A review, Ultrason. Sonochem. 70 (2021) 105293, https://doi.org/10.1016/j.ultsonch.2020.105293.

[29] Y. Ben-Fadhel, B. Maherani, J. Manus, S. Salmieri, M. Lacroix, Physicochemical and microbiological characterization of pectin-based gelled emulsions coating applied on pre-cut carrots, Food Hydrocolloids 101 (1) (2020), 105573, https://doi.org/10.1016/j.foodhyd.2019.105573.

[30] D. D. Li, N. Yang, Y. Tao, et al, Induced electric field intensification of acid hydrolysis of polysaccharides: Roles of thermal and non-thermal effects, Food

Hydrocolloids. 101 (2020) 105484, https://doi.org/101:105484. 10.1016/j.foodhyd.2019.105484.
[31] L. Yu, W. Yang, J. Sun, C. Zhang, J. Bi, Q. Yang, Preparation, characterisation and physicochemical properties of the phosphate modified peanut protein obtained from Arachin Conarachin L, Food Chem. 170 (2015) 169–179, https://doi.org/10.1016/j.foodchem.2014.08.047.
[32] H. Liu, H. Zhang, Q. Liu, Q. Chen, B. Kong, Solubilization and stable dispersion of myofibrillar proteins in water through the destruction and inhibition of the assembly of filaments using high-intensity ultrasound, Ultrason. Sonochem. 67 (2020) 105160, https://doi.org/10.1016/j.ultsonch.2020.105160.
[33] C.H. Tang, F. Liu, Cold, gel-like soy protein emulsions by microfluidization: Emulsion characteristics, rheological and microstructural properties, and gelling mechanism, Food Hydrocolloids 30 (1) (2013) 61–72, https://doi.org/10.1016/j.foodhyd.2012.05.008.
[34] L. Feng, X. Jia, Q. Zhu, Y. Liu, J. Li, L. Yin, et a, Investigation of the mechanical, rheological and microstructural properties of sugar beet pectin /soy protein isolate-based emulsion-filled gels, Food Hydrocolloids 89 (2019) 813–820, https://doi.org/10.1016/j.foodhyd.2018.11.039.
[35] H. Hu, X. Fan, Z. Zhou, X. Xu, G. Fan, L. Wang, X. Huang, S. Pan, L.e. Zhu, Acid-induced gelation behavior of soybean protein isolate with high intensity ultrasonic pre-treatments, Ultrason. Sonochem. 20 (1) (2013) 187–195, https://doi.org/10.1016/j.ultsonch.2012.07.011.
[36] Z. Xi, W. Liu, D.J. Mcclements, L. Zou, Rheological, structural, and microstructural properties of ethanol induced cold-set whey protein emulsion gels: Effect of oil content, Food Chem. 291 (2019) 22–29, https://doi.org/10.1016/j.foodchem.2019.04.011.
[37] M. Zhong, F. Xie, S. Zhang, Y. Sun, B. Qi, Y. Li, Preparation and digestive characteristics of a novel soybean lipophilic protein-hydroxypropyl methylcellulose-calcium chloride thermosensitive emulsion gel, Food Hydrocolloids 106 (2020) 105891, https://doi.org/10.1016/j.foodhyd.2020.105891.
[38] B. Panchal, T. Truong, S. Prakash, N. Bansal, B. Bhandari, Effect of water content, droplet size, and gelation on fat phase transition and water mobility in water-in-milk fat emulsions, Food Chem. 333 (2020) 127538, https://doi.org/10.1016/j.foodchem.2020.127538.
[39] J. Li, L. Xu, Y. Su, C. Chang, Y. Yang, L. Gu, Flocculation behavior and gel properties of egg yolk/κ-carrageenan composite aqueous and emulsion systems: Effect of NaCl - ScienceDirect, Food Res. Int. 132 (2020) 108990, https://doi.org/10.1016/j.foodres.2020.108990.
[40] X. Liang, C. Ma, X. Yan, et al., Structure, rheology and functionality of whey protein emulsion gels: Effects of double cross-linking with transglutaminase and calcium, Food Hydrocolloids 102 (2019), 105569, https://doi.org/10.1016/j.foodhyd.2019.105569.
[41] Y. Lu, L. Mao, H. Zheng, H. Chen, Y. Gao, Characterization of β-carotene loaded emulsion gels containing denatured and native whey protein, Food Hydrocolloids 102 (2020) 105600, https://doi.org/10.1016/j.foodhyd.2019.105600.
[42] C. Soukoulis, S. Cambier, L. Hoffmann, T. Bohn, Chemical stability and bioaccessibility of beta-carotene encapsulated in sodium alginate o/w emulsions: Impact of Ca^{2+} mediated gelation, Food Hydrocolloids 57 (2016) 301–310, https://doi.org/10.1016/j.foodhyd.2016.02.001.
[43] W. Liu, H. Gao, D.J. McClements, L. Zhou, J. Wu, L. Zou, Stability, rheology, and β-carotene bioaccessibility of high internal phase emulsion gels, Food Hydrocolloids 88 (2019) 210–217, https://doi.org/10.1016/j.foodhyd.2018.10.012.